

Development of the Southern Coastal Area of the Caspian Sea during the Pliocene–Quaternary According to Biostratigraphic and Magnetostratigraphic Data

V. G. Trifonov^{a, *}, K. Hessami^b, S. V. Popov^c, E. A. Zelenin^a, Ya. I. Trikhunkov^a, P. D. Frolov^a, L. A. Golovina^a, A. N. Simakova^a, A. Rashidi^b, and A. V. Latyshev^d

^a Geological Institute, Russian Academy of Sciences, Moscow, Russia

^b International Institute of Earthquake Engineering and Seismology, Tehran, Iran

^c Paleontological Institute, Russian Academy of Sciences, Moscow, Russia

^d Institute of Physics of the Earth, Moscow, Russia

*e-mail: trifonov@ginras.ru

Received January 3, 2022; revised February 15, 2022; accepted February 25, 2022

Abstract—The paper considers geological structure of the coastal region of the South Caspian, including paleontological and magnetostratigraphic dating of the Neogene–Quaternary deposits. Western and eastern segments of the region between the South Caspian Basin and the Alborz Ridge developed differently in the Late Cenozoic. In the west, marine sediments did not penetrate beyond the coastal plain into the neighboring lowered part of the Alborz Ridge during the Pliocene–Quaternary. This indicates the stability of the marine basin boundary or its expansion due to the abrasion of the Alborz slopes. In the east, a piedmont step emerged, bounded by thrust faults. The marine deposition at the piedmont step occurred in the Miocene. At the end of the Miocene, the marine sediments were folded and eroded. The Akchagylian (Piacenzian–Gelasian) marine sediments accumulated at the northern edge of the piedmont step. The Khazar fault raised these sediments up to 120–150 m and isolated the piedmont step. Thus, the expansion of the Alborz mountain building and the reduction of the South Caspian Basin occurred in the eastern part of the coastal area from the Late Miocene. The differences between the western and eastern segments of the coastal area are related to the development of the South Caspian Basin. Until the Late Miocene, it remained a residual trough of the Paratethys. During the Pliocene–Quaternary, the eastern part was filled with sediments up to 6 km thick and retained the features of a thinned continental crust 30–37 km thick with sedimentary cover up to 16 km thick. The western part of the basin was filled with sediments about 10 km thick and acquired the features of sub-oceanic crust with the Mohorovichich surface at a depth of 28–30 km with a thickness of the sedimentary cover exceeding 20 km.

Keywords: South Caspian Basin, Alborz Ridge, coastal plain, piedmont step, Miocene, Pliocene, Quaternary, Akchagylian

DOI: 10.1134/S0869593822040074

INTRODUCTION

The southern part of the Caspian Sea forms the South Caspian Basin, the recent bottom of which in the west is at the maximum depths of the Caspian Sea up to 980 m below sea level (Fig. 1). Further to the south, the Alborz Ridge with elevations of up to 3500–4000 m is situated. A narrow coastal area covered mainly by the Upper Quaternary sediments extends between the folded-thrust Alborz Ridge and the South Caspian Basin (Fig. 2). This strip varies in width from a few kilometers to 20 km and widens up to 30 km near the city of Rasht in the west and 35 km between the towns of Amol and Sari in the east.

The aim of the paper is to characterize the coastal area and determine the dynamics of its relationships to

the ridge during the Late Pliocene and Quaternary. To determine the evolution of the relations between the South Caspian Basin and the Alborz, it is important to detect the position of Pliocene–Quaternary shorelines at different times on the southern coast of the Caspian Sea. Of particular importance is the distribution of marine sediments of the Akchagylian transgression (Table 1). Until now, the Akchagylian deposits on the southern shore of the Caspian Sea were unknown to the geological community. The closest marine Akchagylian outcrops to the region of our studies were noted in the northern Talesh on the western coast of the Caspian Sea and between the cities of Gorgan and Gonbad-e Kāvus on the eastern coast (Geological Map of Iran, Sheet 1, 1978; Wang et al., 2016; Soltani et al.,

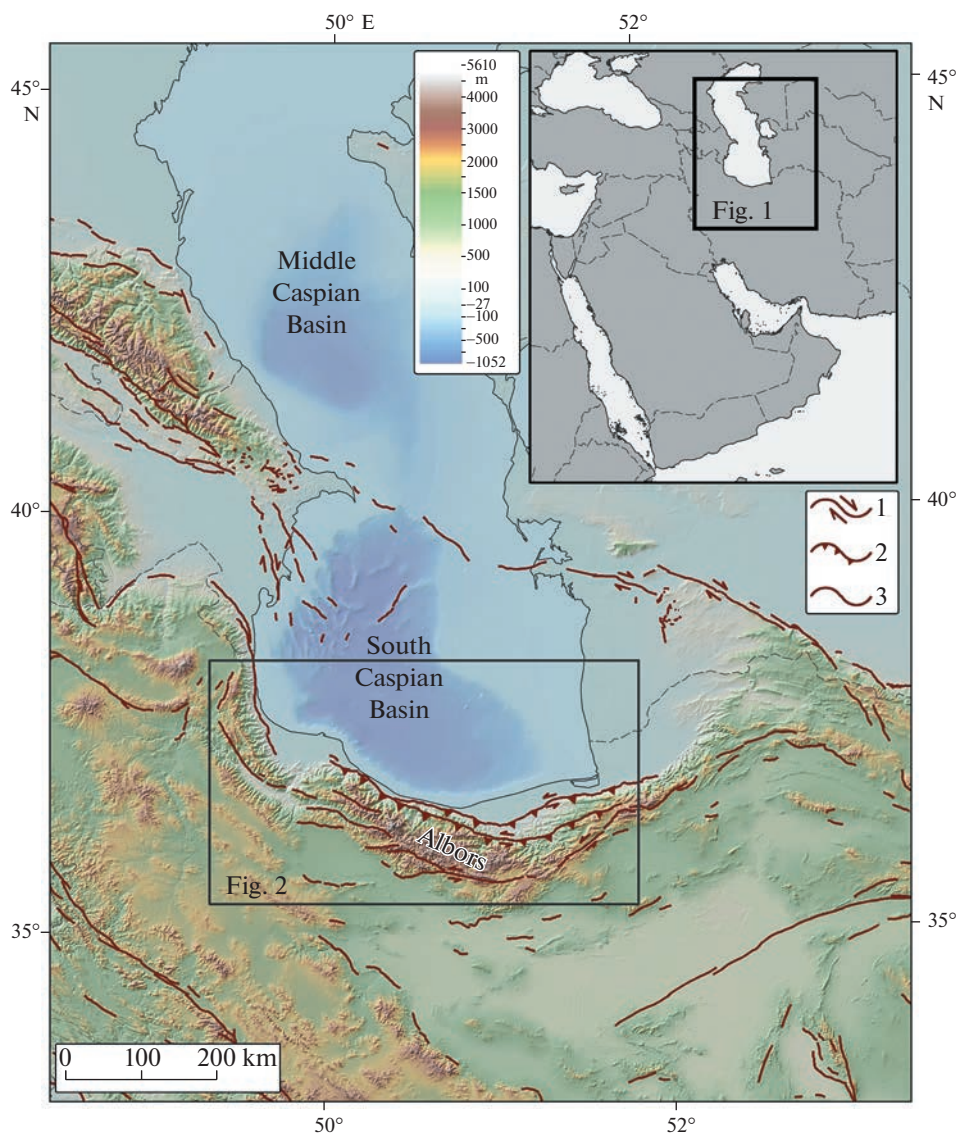


Fig. 1. General topographic map showing position of the studied area (Fig. 2) in the South Caspian–Alborz region and major active faults in this region, after (Trifonov et al., 2002; Talebian et al., 2013). The small map in the upper right corner shows the position of the region in Southwest Asia. (1) Strike-slip fault; (2) thrust or reverse fault; (3) fault with unknown sense of motion.

2020a, 2020b). Only uppermost Pleistocene and Holocene marine sediments have been studied on the southern coast (Svitoch et al., 2013, 2016). Identifying traces of earlier Pliocene–Quaternary transgressions is one of the objectives of this paper.

GEOLOGICAL SETTING

The South Caspian Depression is bounded to the north by the Absheron Sill. According to seismic profiling carried out in the western part of the sill near the Absheron Peninsula, thickening of the sedimentary cover was revealed as result of thrusting of the Middle Caspian crust onto the South Caspian Basin and the related folded-thrust deformation of the sedimentary

cover with predominant southern vergence (Mamedov, 2010; Kangarli et al., 2018). The Mesozoic and Cenozoic rocks up to and including the Miocene are deformed and displaced, whereas the Pliocene–Quaternary sediments covering them with unconformity are much more weakly deformed. The presence of relatively deep earthquakes (50–80 km) and the geometry of the seismic focal zone gave grounds to consider the Absheron Sill as a manifestation of subduction of the South Caspian Basin beneath the Middle Caspian (Ulomov et al., 1999; Knapp et al., 2004). The sill is expressed in the recent structure by a chain of anticlines and an active fault (Fig. 1), which continues eastward by the Isak-Cheleken active dextral strike-slip fault in the Western Kopet-Dag (Trifonov et al.,

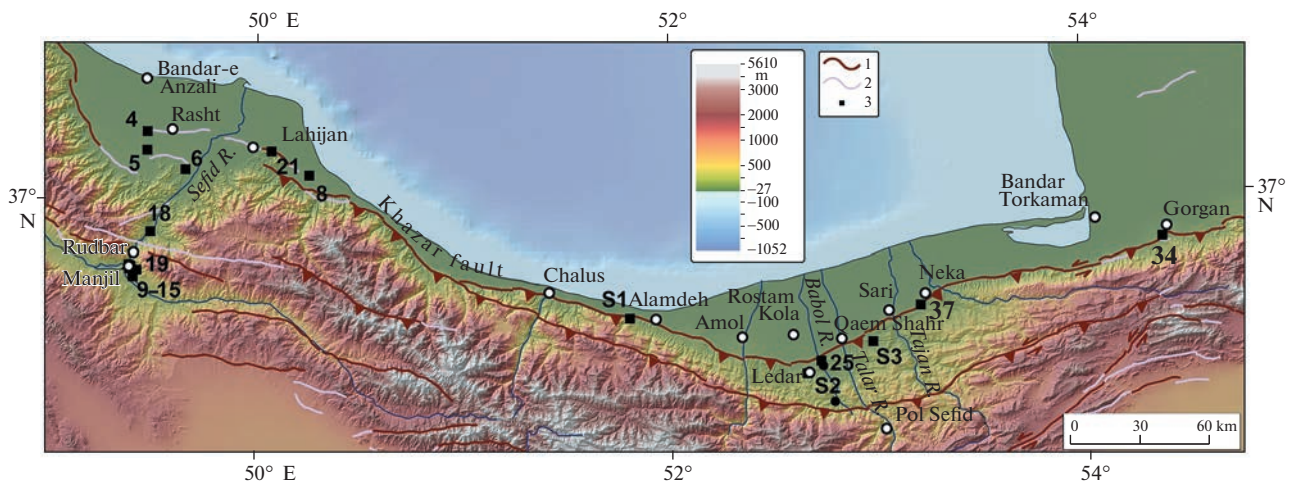


Fig. 2. Topographic map of the coastal area between the Caspian Sea and Alborz and active faults in the region, after (Talebian et al., 2013). (1) Active faults; (2) Pliocene–Quaternary faults; (3) sites of our observations mentioned in the paper. See Fig. 1 for other symbols.

1986; Ivanova and Trifonov, 2002). In the west, the Absheron Sill Fault is continued en echelon by the Main Caucasus active fault zone. Opinions on its kinematics differ. The reverse component of the displacement is undisputed (Trifonov et al., 1996).

Rastsvetaev (1989) noted an echelon location of the NW-trending right-lateral faults along the zone and suggested the presence of the right-lateral component of movements on this zone itself. The Late Cenozoic right-lateral offset on the Main Caucasus fault zone

Table 1. Approximate correlation of the Neogene–Quaternary world stratigraphic scale and the regional stages in the Caucasus-Caspian region discussed in the paper

System	World scale stages		Regional stages	
Quarter-nary	Holocene last 0.0117			
	Upper Pleistocene 0.13–0.0117			
	Middle Pleistocene 0.78–0.13	lower Middle Pleistocene	Bakunian 0.78 to ~0.55	
	Calabrian 1.8–0.78		Apsheonian 1.8* to 0.78	
	Gelasian 2.59–1.8		Akchagylian 3.2* to 1.8	
Pliocene	Piacenzian 3.6–2.59		Balakhanian (Productive) series	
	Zanclean 5.39–3.6			
Miocene	Messinian 7.25–5.35		Pontian ~6.1 to 5.3	
	Tortonian 11.6–7.25		Maeotian ~7.6 to ~6.1	
	Serravallian 13.82–11.6		Sarmatian ~13.0 to ~7.6	
	Langhian 15.97–13.82		Konkian ~13.4 to ~13.0 Karagian ~13.8 to ~13.4 Chokrakian ~14.8 to ~13.8	
	Burdigalian 20.43–15.97		Maykopian Group	Sakaraulian ~20.5 to ~17
	Aquitanian 23.03–20.43			
Oligocene				

The age is shown in Ma. The age of boundaries of the Neogene regional stages is shown after (Popov et al., 2018).

* There is an opinion (Lazarev et al., 2021) that the Apsheonian began ca. 2.1 Ma and the Akchagylian lasted from 2.95 to 2.1 Ma; correspondingly, the upper boundary of the Balakhanian is rejuvenated.

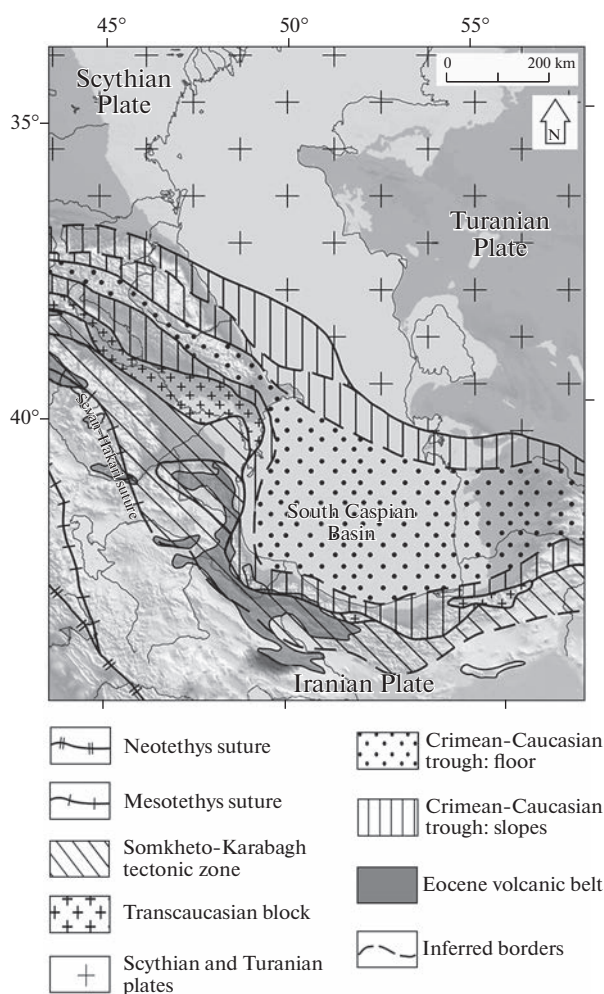


Fig. 3. Mesozoic–Cenozoic tectonic zonation of the Caucasus–Caspian–Alborz region, after (Trifonov et al., 2020) with changes.

and the Absheron Sill Fault by ~100 km is reported in Patina et al. (2017).

The sedimentary cover reaches ~20 km or more farther to the south, in the western part of the South Caspian Basin, 9–11 km of which belongs to the Pliocene–Quaternary and other 9–11 km belongs to the Jurassic–Miocene part of the section (Artyushkov, 1993; Leonov et al., 1998; Brunet et al., 2003; Knapp et al., 2004). This area can be considered as a continuation of the Jurassic–Miocene Caucasus trough, which underwent intense subsidence in the Pliocene–Quaternary (Fig. 3). In the eastern part of the South Caspian and in the West Turkmen Depression, the thickness of the cover is reduced to 16 km owing to thinning of the Pliocene–Quaternary section, whereas the thickness of the Jurassic–Miocene strata is the same as in the western part of the South Caspian (Ivanova and Trifonov, 2002).

The Alborz is a bilateral orogen with a multistage development history (Stöcklin, 1974). The most ancient

metamorphic rocks compose packages of nappes. The age of one of them, east of Rasht, is dated to the Late Ediacaran–Early Cambrian and is similar to rare age determinations of the basement in the Iranian microplate located to the south (Moghadam and Stern, 2014) and is close to the age of the basement of the Dzerulian massif, which is a part of the Trans-Caucasus microplate (Adamia et al., 2017). The traces of the Paleotethys (early Mesotethys) paleo-ocean, which was closed in the Middle Triassic ca. 235 Ma with the collisional orogen formation in the southern side, were found to the west of Rasht and near the city of Mashhad (Sengör, 1984; Alavi, 1996; Zanchi et al., 2006). The collision is fixed by a regional angular unconformity at the base of the Upper Triassic–Middle Jurassic Shemshak Formation.

The Shemshak Formation on the northern slope of the Alborz, near the town of Sari and to the east of it, is dominated by fine-clastic deposits similar to those of the southern slope of the Caucasus Trough (Fig. 3). Coarse sandstones, gravelstones, and carbonaceous shales, similar to the more southern Caucasus zones, appear in the Shemshak Formation south of Rasht (near the town of Rudbar) and on the southern slope of the Alborz (Trifonov et al., 2020). They compose the northern active margin of the Late Mesotethys, often referred to as the northern branch of the Neotethys (Khain, 2001; Sosson et al., 2010). Traces of this paleo-ocean are known in the Lesser Caucasus as the Sevan–Hakari suture (Knipper, 1975; Adamia et al., 2017). Farther, according to Alavi (1996), the suture acquires the character of a transform and follows along the Tabriz (Tabriz–Takestan) fault. The eastern continuation of the suture is hypothetical. It may include a colored melange of Cretaceous age with basalts and ultrabasic bodies, exposed south of the Eastern Alborz between the towns of Forumad and Fariman. The outcrops of melange continue to the SE within the Lut Block and its southeastern rim (Geological Map of Iran, Sheet 3, 1977). The Upper Jurassic–Hauterivian ophiolite Khashrud zone, which is auxiliary relative to the Herat (Main Harirud) fault zone in northwestern Afghanistan, is comparable to the melange (*Geologiya*, 1980).

The Shemshak Formation is overlain with unconformity by shelf sediments, such as limestones of the upper Middle Jurassic, Upper Jurassic, and Lower Cretaceous, Upper Cretaceous marls, and Paleogene sandstones. The Eocene–Oligocene Karaj Formation, composed of subaerial volcanic and tuffaceous rocks, is widespread. Higher is the Upper Red Formation of the Miocene composed of siltstones and sandstones with lenses of gypsum and limestone. The formation of the Alborz folded-thrust structure was completed at the end of the Miocene.

The recent structure of the Alborz develops under transpression (Jackson et al., 2002; Guest et al., 2006). This is evidenced by the kinematics of active faults

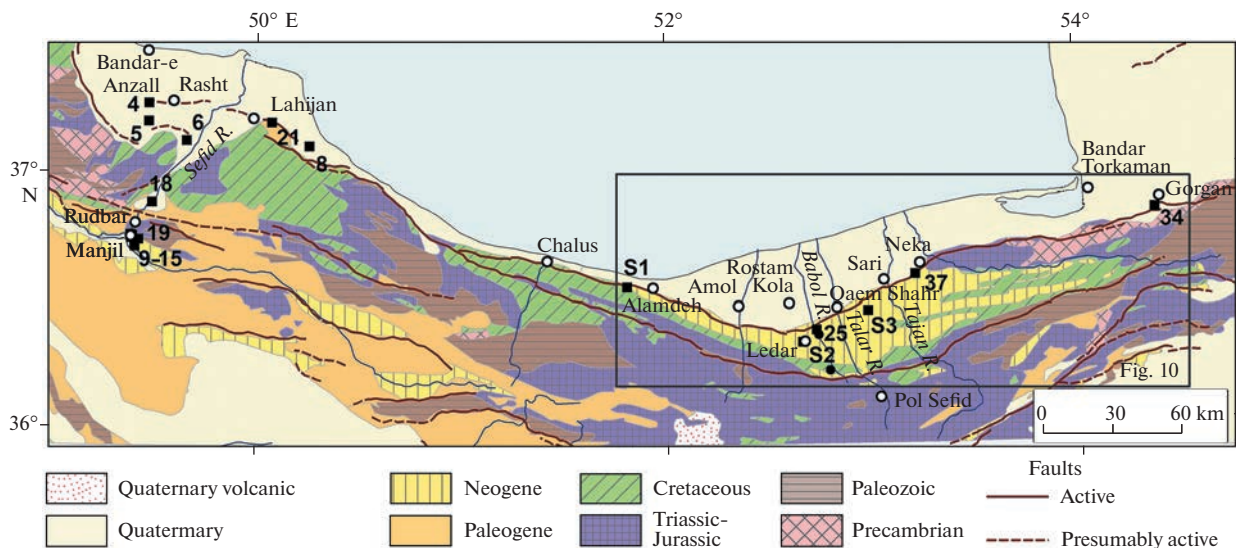


Fig. 4. Geological map of the coastal area and adjacent slopes of the Alborz, simplified after (Geological Map of Iran, Sheet 1, 1978; Sheet 2, 1977).

(Fig. 2). Berberian (1976), who first introduced the active faults, noted the reverse offsets along them. Later on, it turned out that most of the large longitudinal faults of the Alborz and its southern foothills have the left-lateral component of motion, which is close to the vertical component in magnitude or exceeds it (Berberian et al., 1992; Allen et al., 2003; Bachmanov et al., 2004). Allen et al. (2003) considered that the combination of transverse shortening with left-lateral strike slip was characteristic of the entire Late Cenozoic stage of the Alborz development, the beginning of which they presumably attributed to the Middle Miocene. They estimated the Late Cenozoic sinistral strike-slip offset on the Moshafault at 30–35 km, and the total transverse shortening of the ridge at the meridian of Tehran at 30 km, assuming that a part of this shortening could have been realized by the subduction of the South Caspian Basin under the Middle Caspian. The results of GPS measurements confirm the transpression model of the Alborz (Vernant et al., 2004; Djamour et al., 2010; Mousavi et al., 2013; Khorrami et al., 2019). Vernant et al. (2004), on the basis of 2000–2002 geodetic measurements, estimate the present-day N–S-trending shortening rate of Alborz to be 5 ± 2 mm/yr with a cumulative left-lateral slip rate of 4 ± 2 mm/yr. The recent high tectonic activity of Alborz is marked by a number of strong earthquakes with magnitudes M_s up to 7.4.

For the purposes of our paper, the Khazar active fault, which extends along the boundary between the Alborz and the coastal plain (Fig. 4), is particularly important. The fault is divided into the WNW-trending West segment and the ENE-trending East segment. The boundary of the segments is the Babol River valley between the towns of Amol and Sari. Rashidi (2021) separates the Sari segment of the fault

between the Babol River valley and the village of Rostam Kola, where the fault extends to the NE. The western segment of the fault, which Rashidi (2021) calls the North Alborz Fault, is most clearly distinguished. It is ubiquitously expressed in the topography by a scarp (Talebian et al., 2013). Nazari et al. (2021a, 2021b) define the fault as a thrust dipped southward at an angle of $\sim 34^\circ$. The vertical displacement rate is estimated at 2 ± 0.5 mm/yr by the displacement of the dated lower terrace. Accordingly, the horizontal displacement rate along the thrust is ~ 3 mm/yr, and the displacement rate along the uprising of the thrust plane is 3.6 mm/yr. The fault is often hidden under the sedimentary cover and expressed at the surface by near-fault deformation or fault-propagation folds. In the Sari and eastern segments, the fault is hidden, forms a discontinuous series of linear segments, and is expressed by fault-propagation folds (Ghassemi, 2005).

Rashidi (2021) pays attention to the dependence of the character of movements in different segments of the Khazar fault on their strike. While the left lateral strike slip dominates in the ENE-trending eastern segment, it is supplemented by the extension component in the NE-trending Sari segment, and the West (North Alborz) segment is dominated by thrusting. On the basis of block modeling of the results of GPS measurements, Djamour et al. (2010) estimated a left-lateral strike-slip rate for the eastern segment of the Khazar Fault at ~ 5 mm/yr with a transverse shortening rate of 2–3 mm/yr; for the western segment, the left-lateral strike-slip rate is reduced to 1.8 mm/yr with a shortening rate of ~ 6 mm/yr. Recent GPS measurements (Khorrami et al., 2019) indicate that, in the eastern Alborz, strike-slip motion is predominant and occurs at a rate of about 8 mm/yr along the NE trending left lateral faults, while mountain-normal shortening

occurs at a rate of ~2 mm/yr along thrusts. However, in western Alborz, left lateral motion occurs at a rate of ~5 mm/yr along the NW faults, and mountain-normal shortening occurs at a rate of ~5–7 mm/yr along thrusts.

METHODS OF STUDY

The paper is based on fieldworks carried out by S.V. Popov and L.A. Golovina in 2013 and by an Iranian–Russian group consisting of V.G. Trifonov, K. Hessami, P.D. Frolov, A. Rashidi, A.N. Simakova, Ya.I. Trikhunkov, and E.A. Zelenin in 2018. During the fieldworks and processing of the obtained materials, sections of Neogene–Quaternary deposits were described, mollusk and microfossil remains were selected and determined, and samples for magnetic stratigraphy analysis, deformations of these deposits, and structure and evolution of the Alborz –coastal plain border were identified and determined. Paleontological finds were studied at the Paleontological and Geological Institutes of the Russian Academy of Sciences (RAS). Marine mollusk fossils were analyzed by S.V. Popov. P.D. Frolov examined terrestrial Quaternary mollusks. L.A. Golovina studied microfossils. A palynological analysis carried out by A.N. Simakova did not show positive results.

Paleomagnetic samples were manually taken and oriented using a magnetic compass. Samples from loose deposits were strengthened by a nonmagnetic silicate glue. The local magnetic declination was calculated using the IGRF model. The paleomagnetic procedures were performed in the laboratory of paleomagnetism of the Institute of Physics of the Earth, Russian Academy of Sciences, by A.V. Latyshev. All the samples were subjected to the stepwise alternating field (AF) demagnetization up to 130 mT with an AF demagnetizer built into the 2G Enterprises cryogenic magnetometer. The remanent magnetization of samples was measured using a 2G Enterprises Khramov cryogenic magnetometer. The isolation of the natural remanent magnetization (NRM) components was performed with Enkin's (Enkin, 1994) paleomagnetic software package using principal component analysis (Kirschvink, 1980). The results of AF demagnetization of samples, representing all sections where the paleomagnetic samples were collected, are shown in Fig. 5.

The following abbreviations are used in the paper: s—site of studies; a.s.l.—above World Ocean level; H—height a.s.l. All sections are described from the bottom up.

RESULTS

The structure of the coastal plain and its relationships to various elements of the Alborz structure were investigated in the area around the city of Rasht and between the village of Alamdeh and the city of Gorgan.

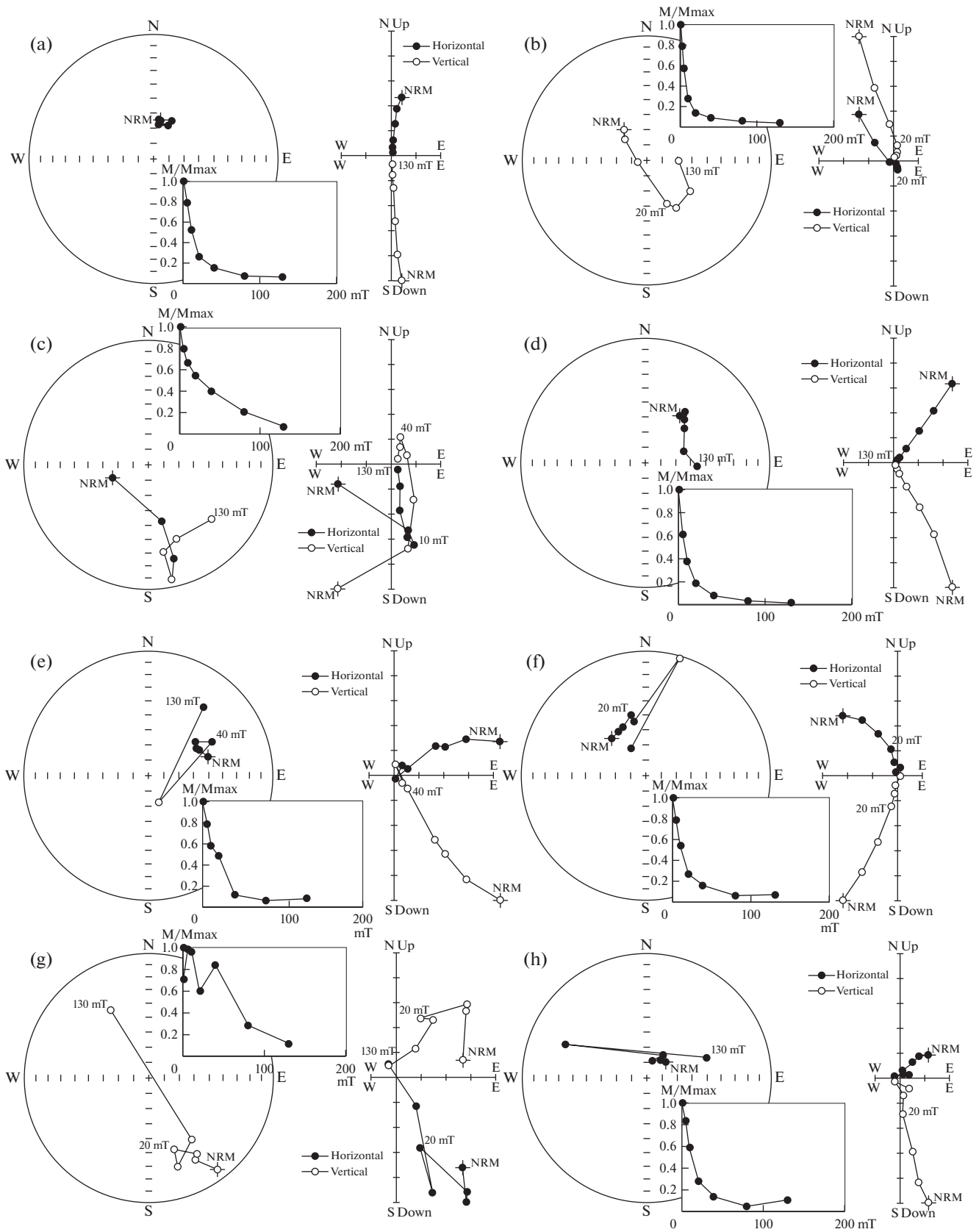
Region of the City of Rasht

The surface of the coastal plain generally gently rises toward the mountains from the present-day shoreline of –26 m to ~10 m a.s.l. The plain is poorly differentiated in elevation. The incisions of recent rivers are extremely small. West of Rasht, the near-surface part of the plain is composed of lagoon type clays (s 5). The results of drilling carried out in 1945–1946 near Bandar-e Anzali demonstrated the presence of Pleistocene marine sediments. The borehole was stopped at a depth of 300 m in a thick stratum of Bakunian (?) marine sediments (Saidov and Kuchapin, 1955).

The coastal plain is ruptured by longitudinal faults and in places separated by faults from the mountain slope. The faults are expressed by rectilinear surface scarps. One of these faults strikes to the SE and in s 4 forms a smoothed scarp with the south side uplifted by 5–6 m. The gradient of the longitudinal profile of the stream flowing from the mountains to the sea increases sharply at the intersection with the scarp. The fault is traced to the SE to the Sefidrud River. On its west bank, the fault bounds the coastal plain and is expressed by folding of the southern side, in which the Jukul Bandan section is described (s 6, 37.12297° N, 49.661202° E; H = 90 m):

1. Alternating interbeds of medium- and coarse-grained sands up to 0.7 m thick. In the upper third of the sequence, silt interbeds (thickness is 0.1–0.3 m) appear. The roof of the bed is undulating, possibly eroded. The total visible thickness is 10–12 m.
2. Thin-layered silt with ferruginate spots and a 0.2 m coarse sand interbed in the roof. The thickness is 0.6 m.
3. Thinly laminated brown clays with thin (up to 1 cm) marl interbeds and a silt interbed with ferruginate spots at 0.6–0.4 m from the roof. The thickness is 2.1 m.
4. Silt similar to the interbeds at the upper part of layer 1, with interbeds of fine-grained sand (0.1 m) at the base and roof. The thickness is 0.4 m.
5. Well-rounded flattened pebbles. The thickness is 2 m.
6. Sand, passing into recent soil in the upper part. The thickness is around 3 m.

Fig. 5. Results of the AF demagnetization: representative stereoplots, Zijderveld plots, and demagnetization paths. Stratigraphic coordinate system; black dots in the stereoplots mean lower hemisphere; empty dots, upper hemisphere. (a) Sample 8, section 9 Manjil; (b) Sample 32, section 9 Manjil; (c) Sample 39, section 9 Manjil; (d) Sample 48, section 9 Manjil; (e) Sample 84, section 6 Jukul Bandan; (f) Sample 94, section 34 Sa'dābād; (g) Sample 99, section 37 Surak; (h) Sample 112, section 37 Surak. Position of the samples is shown in the corresponding stratigraphic columns.



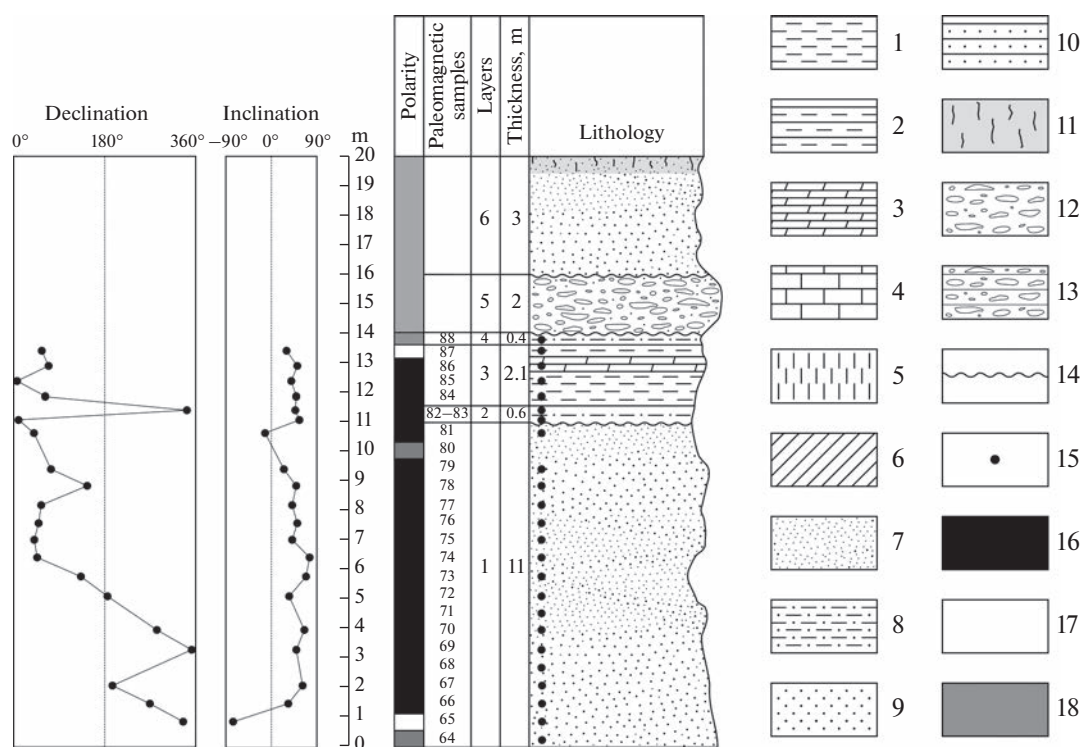


Fig. 6. The Quaternary Jukul Bandan section (s 6). (1) Clay; (2) argillite; (3) marl; (4) limestone; (5) loess; (6) loam; (7) aleurite; (8) aleurolite; (9) sand; (10) sandstone; (11) soil and paleosoil; (12) pebble and gravel; (13) conglomerate; (14) unconformity; (15) place of selection of paleomagnetic sample (16) normal magnetization; (17) reverse magnetization; (18) magnetization unknown.

According to the composition of deposits and characteristics of bedding, the described section (Fig. 6) represents the deltaic deposits of the high terrace of the Sefidrud River. Judging from the relatively weak consolidation of the sediments, we suppose the section belongs to the Quaternary. Most of the section shows normal magnetization, but the presence of reverse polarity layers in the upper and, perhaps, lower parts of the section indicates that it can be attributed to the Lower Pleistocene. The section may correlate with the Jaramillo or Olduvai Subchrons of normal polarity and neighboring intervals of the Matuyama Chron; i.e., it may belong to the Calabrian or even the uppermost Gelasian.

Upstream of the Sefidrud River, the following section (s 18; 36.881096° N, 49.496066° E; H = 166 m) is described on the western side of the valley:

1. Eocene andesitic porphyrites. Visible thickness is 4 m.

2. A lens of gypsiferous silt, similar to some layers of the Upper Pliocene Manjil section (s 9). The thickness is up to 1 m.

3. Pebbles to boulders, overlapping beds 1 and 2 with unconformity. The thickness is 20–30 m. The pebbles are well rounded, consist mainly of volcanic rocks, and represent the channel facies of alluvium.

4. A lens of brownish sandy loam and loam with pebble interlayers. The thickness is up to 4 m. The lens wedges out to the south; to the north, it is partly wedged out and partly replaced by pebbles of layer 5.

5. Pebbles, dark, layered, well- to medium-rounded. The thickness is 7–10 m.

6. Fine-clastic sediments, including loess-like loams. The thickness is up to 4 m.

The sediments of section s 18 compose the high terrace of the river. Layers 3–6 are weakly cemented and, probably, belong to the Quaternary.

Further to the south, a large intermontane basin of the Manjil Reservoir is situated. It is bounded to the north by the W–E-trending (to NW–SE) fault. The rocks are schistose, brecciated, and altered to the green-shale phase of metamorphism in the fault zone (s 15). The breccia contains fragments of metamorphosed basites. The fissility is steeply dipped and oriented along the fault. Red-colored sandstones, gravelites, and less frequently conglomerates and clay shales correlated to the Miocene Upper Red Bed Formation are exposed near the fault on the northern side of the basin (s 12; Fig. 7). Above that, a thick clastic sequence fills the basin. In its eastern part south of the town of Manjil (s 9; 36.7073° N, 49.414922° E; H = 346 m to 36.708609° N; 49.419672° E), the section is as follows (Fig. 8):



Fig. 7. The Upper Red Bed Formation near the fault in the northern side of the Manjil Basin (s 12).

1. Siltstone splintery fractured, bedded, with thickness of interbeds of 0.2–0.5 m. The visible thickness is 6 m.

2. Medium-grained sandstone. The thickness is 0.9 m.

3. Siltstone similar to layer 1. The thickness is 3.5 m.

4. Fine- to medium-grained sandstones, flaggy, with ripple marks. The thickness is 27 m. Interbeds of greenish argillite 7 m from the roof (20 cm) and at the top (5 cm) of the stratum.

5. Splintery fractured siltstone with dense interbeds up to 0.2 m thick and interbeds of flaggy fine-grained sandstone up to 0.5 m thick. The thickness is 40 m.

6. Layered conglomerates with pebbles of varying rounding and different size, with a sandy matrix and sand interbeds. The thickness is up to 50 m.

To the east (s 14 and farther to the south), pebble interbeds appear in layer 5, which is covered by a less consolidated boulder and pebble sequence, probably correlated to layer 6 of s 9; individual boulders reach 1 m across; thickness is 15–20 m.

According to the composition of deposits and characteristics of bedding, layers 1–5 of the section described are lacustrine and alluvial sediments, considerably more consolidated than those of s 6 and s 18. These sediments lie above the Miocene Upper Red Bed Formation and are overlain by the less compacted boulder-conglomerate layer 6, which is similar to the Quaternary sediments of s 18. Therefore, we presumably attribute strata 1–5 of the s 9 section to the Pliocene. No biotic records were found in layers 1–5. They show mostly normal magnetic polarity with two intervals of reverse polarity. We presumably correlate these layers to the Gauss Chron with the Kaena and Mammoths Subchrons, i.e., to the Upper Pliocene.

Near the northern boundary fault, the layers of the red-colored and s 9 formations dip steeply to the south. To the south, the beds of the s 9 Formation are increasingly flattened. In a large part of the basin, they lie horizontally or dip very gently to the center of the basin. North of the s 9 section, layers form a gentle anticline. In s 10, there is a thrust dipping northward at an angle of 30° and accompanied by a near-fault deformation (Fig. 9).

In the NE of the basin, on the eastern bank of the Manjil Reservoir (s 19), three terraces are identified on the surface of the layers described in s 9. The upper terrace is covered by a layer of pebbles 1 m thick. The other two terraces are erosional. Probably, they reflect the phases of fall of the lake level during the final (Quaternary) stage of its existence within the basin. Deposits similar to layers 1–5 of s 9, which compose the basement of these terraces, are inclined at an angle of 5° relative to their surface.

So, in the section of the Caspian coast south of the city of Rasht, the Pliocene–Quaternary deposits within the Alborz Ridge are represented by alluvial and lacustrine facies. Marine sediments are found only within the coastal plain. A significant part of the coastal plain–mountain boundary is formed by faults with the uplifted mountain side, but in places it is an erosion scarp. The piedmont that can be interpreted as a result of spreading of mountains is absent in the Alborz northern slope. Its small heights near the coastal plain are the result of erosion. Such relationships indicate the permanence of the marine basin–ridge boundary or advance of the sea to the mountains with coastal abrasion.

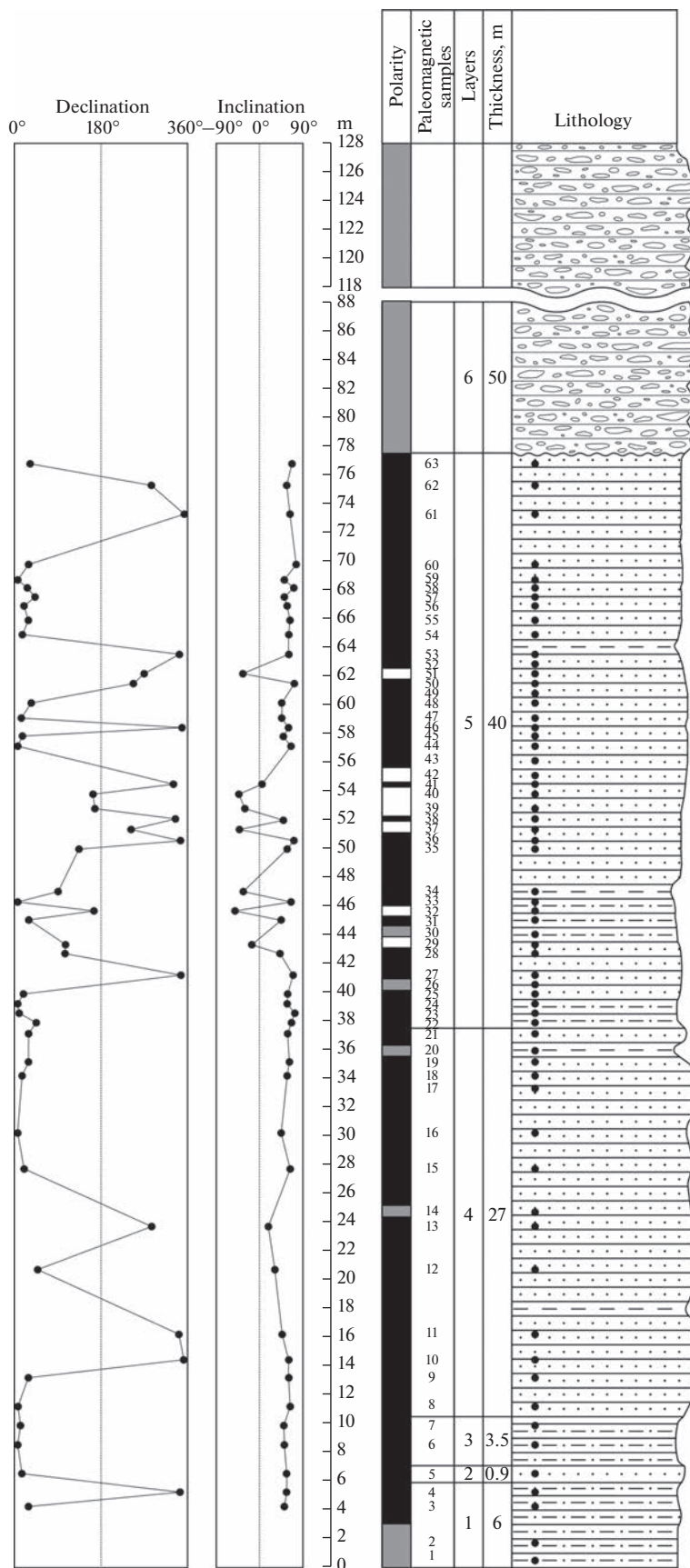


Fig. 8. The Late Cenozoic Manjil Basin section (s 9). See Fig. 6 for the legend.



Fig. 9. The thrust in the Manjil Basin deposits to the south of the town of Manjil (s 10).

The Region between the Village of Alamdeh and the City of Gorgan

The coastal plain narrows sharply in the east of the described part of the coast. At the western end of the Khazar Fault scarp east of the town of Lāhijān, a rocky outcrop of Permian (Geological Map of Iran. Sheet 1, 1978) limestone is broken by fractures (s 21). The fractures striking along the fault and dipping to the south show oblique striation, indicating a combination of left-lateral strike slip and dip slip on the fault. To the southeast, near the village of Shalmān (s 8), a narrow floodplain of a small river is displaced on the fault by 0.5 m vertically; the southern flank is raised. The narrow coastal plain, bounded by the Khazar Fault, extends to the town of Chālus. Eastward, as the coastline recedes from the fault, the coastal plain widens up to 35 km between the towns of Āmol and Qaemshahr. Farther to the east, the Khazar fault gradually converges with the Caspian shoreline, and the width of the coastal plain is reduced to 5–10 km near the city of Gorgan.

Marine sediments other than Holocene beach sediments were not found in the coastal plain. However, a borehole drilled in the town of Bandar Torkaman on the southeastern edge of the South Caspian Basin in 1945–1946 uncovered marine sediments over 1000 m thick (Saidov and Kuchapin, 1955). The quoted authors attributed these sediments to the Bakunian regional stage (lower Middle Pleistocene), but, most likely, the Lower Pleistocene is also present among them.

In the coastal area under consideration, the coastal plain is located at heights from the current level of the Caspian Sea (–26 m) to 40 m a.s.l., rising southward

owing to the alluvial fans of watercourses of different sizes. The eastern part of the Alborz is characterized by elevations ranging from 1200 m on the northern slope to 3000 m at the axial part. Between the ridge and the coastal plain, a piedmont step stands out. Its summit plain, dissected by river valleys, ranges from ~200 m to 1000 m a.s.l., generally rising to the south (Fig. 10). The piedmont step is separated from the mountain ridge by a scarp of a recent fault that has a thrust component of movement. To the north of the town of Pol-e Sefid, the marbled Jurassic limestones of Alborz are gently thrust onto the Cretaceous deposits of the piedmont step (Saidov and Kuchapin, 1955).

The piedmont step is composed of Cretaceous, Miocene, Pliocene, and Quaternary rocks (Fig. 11). Golubyatnikov (1921), who visited the region in 1916, first noted the existence of Miocene and Akchagylia fauna within the step. Later a group of Soviet scientists studied the Cenozoic stratigraphy of the region in detail and compiled the Geological Map of Tertiary Deposits of the Mazandaran Province of Iran at 1 : 200000 scale in 1945–1946. The results of this work, published in a book (Saidov and Kuchapin, 1955), remained unknown to the international geological community, including Iranian geologists. Subsequent Iranian geological maps are characterized by worse stratigraphic differentiation and, accordingly, depiction of the structure. The book (Saidov and Kuchapin, 1955) served as the basis for the stratigraphic and paleontological study of the region carried out by Popov and Golovina (2015). As a result, the section of the piedmont step sediments appears as follows.

Cretaceous deposits that cover marbled limestones of the Upper Jurassic: (1) sandstones and clays,

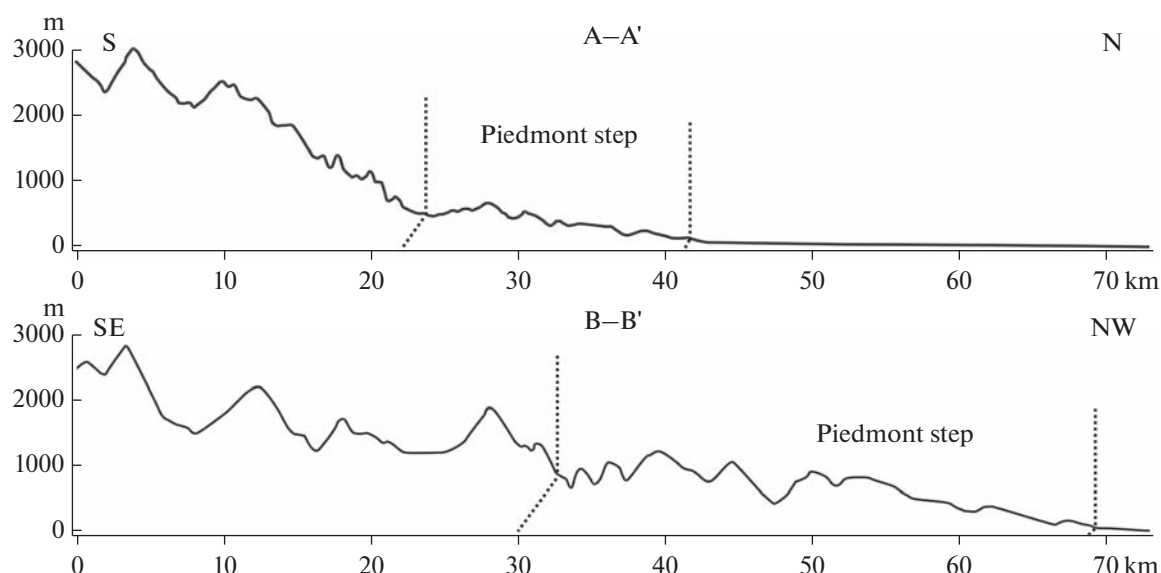


Fig. 10. Geomorphological profiles across the coastal area and piedmont step between the village of Alamdeh and the city of Gorgan. Position of the profiles is shown in Fig. 11.

thickness of ~400 m; (2) limestones with conglomerates at the base and Aptian–Albian *Inoceramus* fauna, thickness of 700–800 m; (3) sandstones and clays with conglomerate interbeds and *Inoceramus* shells and foraminifers of Campanian–Maastrichtian in the lower part and interbeds of limestone and foraminifers of Danian in the upper part, thickness of 200–250 m.

Lower Miocene clays with sandstone interlayers, covering the Cretaceous deposits with unconformity. The found mollusks *Fragum semirugosum* (Sandberger), *Laevicardium spondyloides* (Hauer), *Anadara sakaraulensis* (Popov), *Glossus humanus* (Linnaeus), *Callista lilacinoides* Schaffer, *Calistotapes vetula* (Basterot), *Dosinia exoleta* (Linnaeus), and *Lyonsia macai* Kharatishvili are typical of the Sakaraulian regional stage (20.5–19 Ma), i.e., the upper part of the Maikopian Group. The nannoplankton *Triquetrorhabdulus challengerii* Perch-Nielsen and *Sphenolithus conicus* Bukry are found in these deposits. The first species has the stratigraphic range within the Lower Miocene zones NN1–NN2. The thickness is ~100 m.

The Middle Miocene is represented by the Chokrakian, Karaganian, Konkian, and Sarmatian regional stages.

The **Chokrakian** is characterized by facies variability and is composed in some places of marine clays, sandstones, marls, and limestone, and in others, it is composed of red-colored sandstones and silts of fluvial origin. Among the bivalves and gastropods found in marine sediments, the indicative forms of the lower Chokrakian *Mytilus fuscus* M. Hoernes, *Macoma sokolovi* Bajarunas, *Parvicardium* cf. *michelotti* (Deshayes), *Pitar* cf. *rudis* Poli, *Chlamys* (*Aequipecten*) cf. *opercularis* Linnaeus, *Atamarcia taurica* (Bajarunas), *Gibbula* cf. *kert-*

chensis (Uspenskaya) [after (Saidov and Kuchapin, 1955) in the revised nomenclature] are identified. The thickness is up to 100 m.

The **Karaganian** is composed of siltstones with interbeds of sandstone and limestone in the upper eastern sections. The lower substage is distinguished by the presence of numerous *Davidashvilia* (*Zhgentiana*) (= *Spaniodontella*) *gentilis* (Eichwald) and rarer gastropods of the genus *Rissoa* (*Mohrensternia*). The upper substage is present also, being identified by finds of specific form of genus *Savanella*. The thickness varies from 74 to 110 m and more.

The **Konkian** was probably mainly eroded by the Sarmatian transgression. Its remains are composed of clays with interbeds of sandstone and, less frequently, limestone and are represented only by Barnean layers with *Barnea uiratamica* (Andrussow), *B. ustjurtensis* (Eichwald) and ?*Ervilia* sp. The thickness is 78 m in a borehole near the town of Qaemshahr.

The **Sarmatian** is most widespread within the piedmont step and is represented by the lower, middle, and, possibly, upper substages. The Lower Sarmatian is composed of alternating clays and sandstones with interbeds of limestone. The thickness varies from 70–75 m to 100–140 m. The sandstones of the Lower Sarmatian of the Babol and Talar Rivers contain forms characteristic of the semi-enclosed Sarmatian basin: *Maetra eichwaldi* Laskarev, *M. andrussovi* Kolesnikov, *Musculus* cf. *sarmaticus* (Gatuev), *Plicatifformes praeplacata* (Hilber), *P. plicata* (Eichwald), *Obsoletiformes lithopodolica* (Dubois), *Venerupis* (*Polittapes*) *vitaliana* (Orbigny), *Gomphomarcia naviculata* (R. Hoernes). Along with them, *Tellina* (*Laciolina*) cf. *pretiosa* Eichwald and *Varicorbula gibba* Olivi were found,

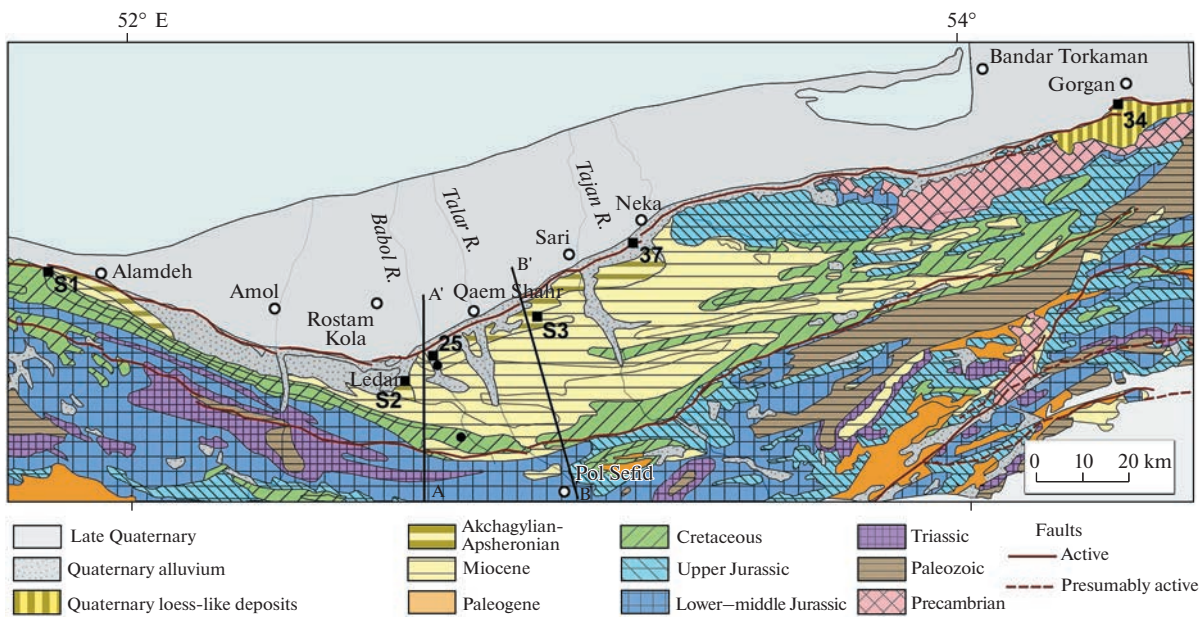


Fig. 11. Geological map of the coastal area and piedmont step between the village of Alamdeh and the city of Gorgan, after (Geological Map of Iran, Sheet 2, 1977; Saidov and Kuchapin, 1955) with changes.

which are absent in the Sarmatian of other regions of the eastern Paratethys and are known only in more euhaline sediments. Nannoplankton is represented by *Coccolithus pelagicus*, *Helicosphaera carteri*, *Sphenolithus* sp., *Reticulofenestra* sp., *Calcidiscus leptoporus*, *Discoaster deflandrei*, and *Coccolithus miopelagicus*. The last two species of mollusks and the relatively diverse composition of nannofossils indicate the influence of the communication channel with the open sea waters of the Mediterranean and/or the Indian Ocean.

The Middle Sarmatian is composed of alternating siltstones and sandstones, with sandstones predominating in the upper sections of the Tajan River. There are interbeds of limestone and lignite. The thickness increases from west to east from 130 m near the village of Alamdeh to 450 m between the Tajan River and the town of Neka. Together with typical Middle Sarmatian forms *Maetra* ex gr. *vitaliana* (Orbigny), *M. andrussovi* Kolesnikov, *Donax dentiger* Eichwald, *Plicatifformes plicata* (Eichwald), *Obsoletiformes* sp, *Venerupis (Polititapes) vitaliana* (Orbigny), *Gomphomarcia naviculata* (R. Hoern.), and *Solen* sp., the relatively euhaline *Parvicardium* ex gr. *exiguum*, *Cultellus* sp., and *Varicorbula gibba*, unknown in the typical Middle Sarmatian, are found. In the same layers, nannoplankton *Reticulofenestra* sp., *Coccolithus pelagicus*, *Helicosphaera carteri*, and *Sphenolithus* sp. were determined, which also indicates the entry of marine water masses from open basins.

The Upper Sarmatian distinguished only presumably because of scanty paleontological substantiation. Saidov and Kuchapin (1955) reported an alternation

of clays, sandstones, and conglomerates up to 200 m thick to the west of the Talar and Tajan River watershed. The content of conglomerates decreases to the north.

In the northeast of the piedmont step, a band of Upper Jurassic marbled limestone and ancient metamorphic rocks is situated. The latter can be dated to the Late Ediacaran–Early Cambrian by analogy with the metamorphic rocks near the town of Lāhijān in West Alborz and the Torud-Biarjmand area (Moghadam and Stern, 2014). The structural relationships of the Jurassic and ancient rocks to the deposits of other parts of the piedmont step are unclear; the Geological Map of Iran, Sheet 2 (1977) shows the transgressive overlap of the Cretaceous deposits on them.

The Cretaceous and Miocene deposits of the piedmont step were deformed into W–E-trending linear folds at the end of the Miocene. At the same time, the northeastern part of the future piedmont step, where its highest peak (1269 m) is located, was probably raised. In the Early Pliocene, during the significant fall of the Caspian Sea level, the anticlines elevated in the relief were eroded, and the waters of the Akchagyalian transgression of the Caspian Sea penetrated to the leveled surface of the northern edge of the piedmont step. The most complete Akchagyalian section is described by Saidov and Kuchapin (1955) near the Khazar fault south of the village of Alamdeh (s S1; 36.551308° N, 51.807847° E; H = 153 m):

1. Bedded clays and siltstones with thin interbeds of sandstones and marls, covering the Sarmatian deposits with unconformity and containing the mollusk fauna:

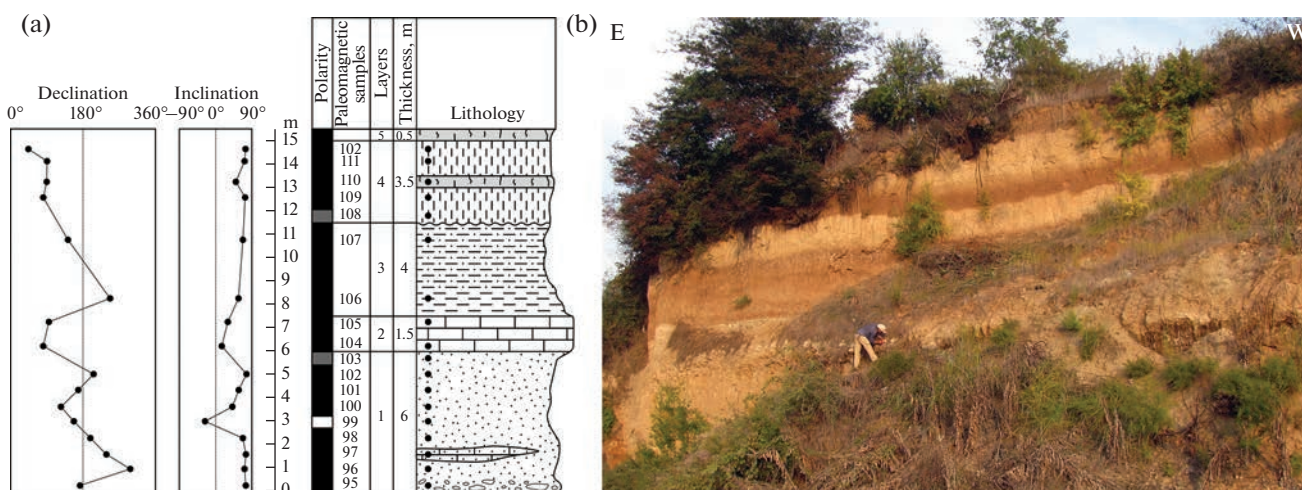


Fig. 12. The Akchagylian section (s 37) near the town of Surak. (a) Stratigraphic column, (b) photo). See Fig. 6 for the legend.

Aktschagylia karabugasica (Andrussow) and *A. venjukovi* (Andrussow). The thickness is 200–250 m.

2. Alternating siltstones, coarse sandstones and conglomerates to boulders. The thickness is 45–50 m. The siltstones of the lower part contain many fragments of cardiums and dreissenids.

3. Siltstones with mollusk fauna: *Cerastoderma* cf. *dombra* (Andrussow), *Aktschagylia karabugasica*, and *A. venjukovi*. The thickness is 35–40 m.

The Akchagylian deposits upward are replaced by clays and siltstones with rare and thin interbeds of medium-grained and coarse sandstone and rare carbonate concretions; thickness is 250–300 m. A 50-m-thick bed of conglomerate with pebbles of Jurassic and Cretaceous rocks lies at the base. The clays and siltstones contain small shells of gastropods and pelecypods, among which the Apsheronian form *Apscheronia colvenscens* Andrussow, *Monodacna* sp., and *Dreissena* sp. were identified (Saidov and Kuchapin, 1955).

The Akchagylian sandstones were found in the Sajjad River valley near the village of Ledar (s S2). The large field of Akchagylian sandstones extends from the left bank of the Talar River, 3 km SW of Qaemshahr, eastward into the valley of the Siah River to the village of Reykandeh (s S3; 36.450158° N, 52.975658° E; H = 110 m). The mollusks *Valvata?* sp., *Potamides caspius* Andrussow, *Aktschagylia subcaspia* (Andrussow), *A. karabugasica*, *A. venjukovi*, and *Cerastoderma dombra* were found [Here and in the section of s S1, the list of mollusks is given after (Saidov and Kuchapin, 1955) in the revised nomenclature (Danukalova, 1996)]. Further to the east, the Akchagylian deposits were noted to the east of the town of Sari in the scarp of piedmont step. Near the village of Surak (s 37; 36.588845° N, 53.210283° E; H = 45 m), the Akchagylian deposits are exposed in near-horizontal position (Fig. 12):

1. Fine-grained, bedded sands with interbeds of pebbles in the lower part and lenses of carbonated

sandstone. The pebbles consist of rounded fragments of Upper Jurassic limestone. Visible thickness is 6 m.

2. Limestone. The thickness is 1–1.5 m.

3. Greenish gray clays and loam, transitioning to brown ones along an irregular boundary. The thickness is 4 m.

4. Loess-like loam with an interbed (to 0.5 m) of dark brown paleosol. The thickness is 3–3.5 m.

5. Recent soil. The thickness is up to 0.5 m.

All deposits of the section show normal magnetic polarity, except a short reverse interval within layer 1. We presumably correlate layers 1–3 to the Gauss Chron and attribute them to the lower Akchagylian (ca. 3.2–2.6 Ma). The loess-like loam 4 can belong to the Brunhes Chron (Middle–Upper Pleistocene).

The marine Akchagylian is unknown in the more southern parts of the piedmont step. In high terraces of large river valleys, the Sarmatian and older deposits are unconformably overlain by alluvial gravels, sands, and loam. For example, in section s 25 (36.378764° N, 52.726878° E; H = 81 m) on the right bank of the Talar River, pebbles over 20 m thick with sandstone lenses cover the eroded surface of Sarmatian siltstones, clays, sandstones, and limestone, dipped northward at 7°–11°. Similar relationships were observed in other valleys of the step (s 27, 28).

Loess-like deposits are exposed on the watersheds. They reach especially high thickness around the city of Gorgan. Near the village of Sa'dābād (s 34; 36.828982° N, 54.382851° E; H = 114 m), the walls of a quarry are composed of 25-m-thick loess-like loam with paleosol horizons and pebble interbeds in the lower part (Fig. 13). The layers very gently dip to the north. Terrestrial mollusks were found in the loam: *Pomatias hyrcanum* (Martens), *Caspicyclotus sieversi* (L. Pfeiffer), *Geminula didymodus* (O. Boettger), *Geminula* cf. *ghilanensis* (Issel), *Drusia ibera*

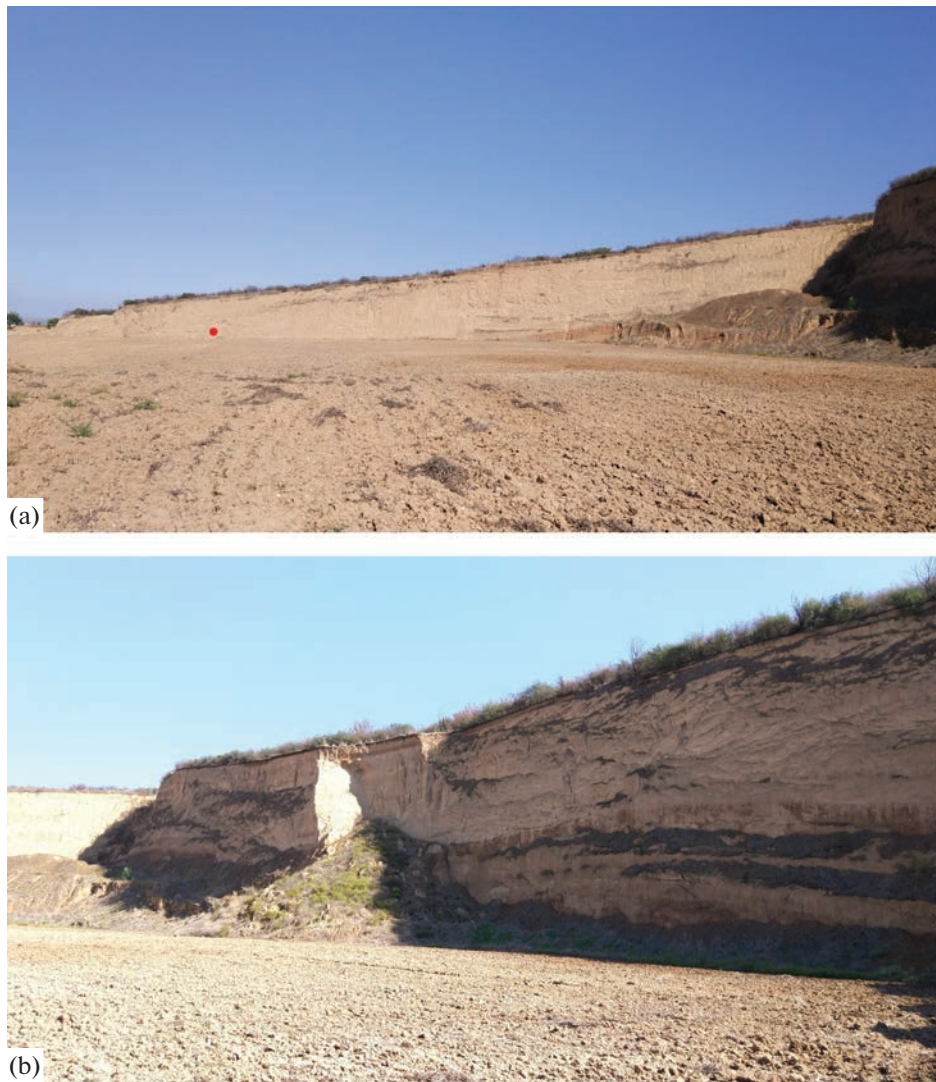


Fig. 13. The loess-soil section 34 near the village of Sa'dābād: views to the northeastern (a) and southeastern (b) walls of the quarry. Red bullet indicates the place of collection of mollusks. The paleomagnetic samples were collected from the southeastern wall.

(Eichwald), *Truncatellina cf. callicratis* (Scacchi), *Gibbulinopsis cf. signata* (Mousson). This complex shows a mixed association of forest species (*Pomatias*, *Caspicyclotus*) and species preferring open slopes and steppe and mountain-steppe areas. All these species still live in this region (Schileyko, 1984; Sysoev and Schileyko, 2009; Bank and Neubert, 2016). The lower 6 m of the section show normal magnetic polarity. Vlamincik et al. (2016) attribute the neighboring (~4 km to the east) loess-soil Toshan sequence to the Upper Pleistocene on the basis of luminescence dating and correlation to other loess-soil sequences in the region.

Loess-like deposits extend farther to the northeast. Near the town of Gonbad-e Kāvus, Wang et al. (2016) dated the oldest loess formation at ca. 2.4–1.8 Ma and found limestone 2–3 m thick in its base with impres-

sions and casts of mollusks. Among them, G.A. Danukalova identified characteristic Akchagylian forms: *Aktschagyliya subcaspia*, *A. cf. ossoskovi* (Andrussow), *A. cf. karabugasica*, *Cerastoderma cf. dombra*, *C. cf. altum* (Tscheltzov) (Wang et al., 2016).

Thus, in the coastal area under consideration, the marine basin spread in the Early and Middle Miocene at least up to the southern margin of the recent piedmont step. In the Late Miocene, the accumulated sediments were folded. In the Early Pliocene, the deformational uplifts were eroded to such an extent that the Akchagylian marine deposits up to 320 m thick were accumulated on the northern part of the piedmont step. In a more limited area (at least to the south of the village of Alamdeh), marine sedimentation continued during the Apsheronian, when up to 300 m of sedi-

ment was deposited. In the more southern parts of the piedmont step, river valleys developed at this time, where pebble to boulder alluvium accumulated, indicating intense uplift and erosion of the Alborz, from which the rivers of the piedmont step flowed.

In the late Early and early Middle Pleistocene, movements on the Khazar fault isolated the piedmont step from the coastal plain, which remained a shallow part of the Caspian shelf at that time. The Akchagylian deposits were partly included in the fault-propagation folds. The height of the maximum Akchagylian transgression did not exceed 40–50 m according to our calculations. Now the Akchagylian sediments of the piedmont step are found at elevations up to 120–150 m a.s.l. This determines the minimum magnitude of the Quaternary vertical offset on the Khazar fault at 60–100 m (without taking into account the subsidence of the coastal plain). Since the Akchagylian marine sediments, up to 300–320 m thick, could not have pinched out suddenly southward, we must assume a thrust overlap of the pinch-out zone on the Proto-Khazar fault.

The Alborz Jurassic deposits are thrust to the piedmont step on the fault zone limiting the step from the south. In a number of places, the folds of the piedmont step are obliquely adjoined to the boundary fault. Apparently, there was a thrust overlap of a part of the southern piedmont step. The age of this displacement cannot be determined accurately. The displacement occurred after the sediments of the piedmont step had been folded, i.e., not earlier than the Late Miocene–Early Pliocene. Probably, the movements continued into the Quaternary.

Thus, the Alborz Ridge expanded at the expense of the reduction of the South Caspian Basin in the eastern part of the southern coast of the Caspian Sea in the Late Cenozoic. So, the development of the region under consideration is fundamentally different from that of the coast in the vicinity of Rasht.

DISCUSSION

The differences in Pliocene–Quaternary development of the western and eastern parts of the southern Caspian coast are related to the differences in the western and eastern parts of the South Caspian Basin. Before the Early Miocene, both parts of the depression were a part of the Black Sea–Caucasus–South Caspian trough of the Paratethys and were characterized by a continental crust with a thick (9–11 km) sedimentary cover and thinned crystalline basement (Trifonov et al., 2020). At the very end of the Miocene and the Early Pliocene, there was a change in the relationships between tectonic zones: transverse tectonic zoning intensified. This was manifested in the start of mountain building in the Greater and Lesser Caucasus and sharp sinking of the western part of the South Caspian Basin and deeper sinking of the Derbent part of

the Terek–Derbent foredeep as compared to its northwestern Terek part. The level of the Caspian Sea decreased sharply in the Early Pliocene. Marine sedimentation continued only in the South Caspian Basin and in the south of the Middle Caspian. In the dried northern part of the Middle Caspian, river valley incisions up to 0.7 km deep occurred, continuing northward (Antipov et al., 1996; Leonov et al., 2005). At the same time, up to 6 km of sediments accumulated in the western part of the South Caspian Basin in the Early Pliocene (Leonov et al., 1998). The accelerated sinking of the western part of the South Caspian compared to its eastern part continued during the Late Pliocene and Pleistocene. As a result, about 10–11 km of Pliocene–Quaternary sediments accumulated in the west of the basin and not more than 6 km accumulated in the east. The eastern part of the basin, which continues into the West Turkmen Depression, retained the features of a thinned continental crust with a total thickness of 30–37 km and a thickness of the cover up to 16 km, but in the western part of the basin, the crust acquired the suboceanic features with a total thickness of 28–30 km and a thickness of the cover of ~20 km (Ivanova and Trifonov, 2002).

A clockwise rotation model of the South Caspian Basin (Jackson et al., 2002; Ritz et al., 2006; Mousavi et al., 2013; Khorrami et al., 2019; Nazari et al., 2021a, 2021b), which agrees with the block interpretation of the GPS observations in the Alborz (Djamour et al., 2010), was proposed to explain the structural relations of the Alborz and the South Caspian Basin. However, this model is contradicted by the data on the active right lateral strike slip along the Absheron Sill, which is the northern boundary of the South Caspian Basin (see Geological Setting and Fig. 1). The right lateral strike slip was also detected on the NW-trending Saliyany-Liangabiz fault zone in the east of the Kura Basin, and N-trending and NNE-trending normal faults extend along the western shore of the South Caspian (Trifonov et al., 2002).

Therefore, arguments in favor of the westward or northwesterly movement of the South Caspian Basin seem more likely (Allen et al., 2003; Vernant et al., 2004; Rashidi, 2021). One may agree with the model of Kopp (1997), according to which the Kopet Dagh orogen, bounded from the north by the Main Kopet Dagh fault of northwestern strike, reacts to the N-trending pressure of the more southern tectonic zones in the Late Cenozoic by transverse shortening and squeezing of the Kopet Dagh crustal masses westward. We assumed that the pressure exerted by such movement on the western part of the South Caspian Basin could have caused metamorphism and, accordingly, compaction of its lower crust, which led to a more intense sinking of this part of the basin. The metamorphosed crustal rocks acquired the density of the mantle rocks, which is expressed in the velocity pattern by the uplift of the Mohorovichich surface.

CONCLUSIONS

The Pliocene–Quaternary development of the southern Caspian coast occurred differently in the western part (the Rasht area) and eastern part (between the village of Alamdeh and the city of Gorgan). In the west, the coastal plain is separated from the Alborz Ridge by scarps, largely formed by active faults. Quaternary and, possibly, Upper Pliocene marine deposits are present only under the coastal plain and do not penetrate into the adjacent lowered part of the Alborz. Only Pliocene and Quaternary fluvial deposits are common there. This indicates the stability of the marine basin boundary or its expansion due to abrasion of the Alborz slopes.

In the east, a piedmont step, the upper surface of which rises from north to south from 200 m to 1000 m, is distinguished between the coastal plain and the Alborz Ridge. The piedmont step is bounded on both sides by faults with thrusting of the southern side. During the Miocene, the marine basin spread southward at least over the entire territory of the piedmont step. The marine sediments were folded into W–E-trending folds in the Late Miocene. In the Early Pliocene, the deformational uplifts were so eroded that, in the zone of the northern boundary Khazar fault and at the adjacent edge of the step, the Akchagylian (Piacenzian–Gelasian) marine sediments up to 300–320 m thick were accumulated. Continued uplift of the southern flank of the Khazar fault separated the piedmont step from the coastal plain. Judging by the present-day bedding of the Akchagylian deposits, the vertical component of displacement on the fault exceeded 100 m. The rear parts of the coastal plain and the piedmont step were partially overlapped by the thrusting along the boundary faults. Thus, there was an expansion of the mountain structure and reduction of the marine basin in the eastern part of the Caspian coast, in contrast to its western part, from the Late Miocene to the present.

The differences in the Late Cenozoic development of the western and eastern segments of the southern Caspian coast are related to the peculiarities of the development of the South Caspian Basin. Until the Late Miocene, the basin remained a single residual trough of the Paratethys. But in the Late Miocene and Pliocene–Quaternary, the differences in the intensity of subsidence and transformation of the crust of the western and eastern parts of the basin clearly emerged. The eastern part was filled with Pliocene–Quaternary sediments up to 6 km thick and retained the features of a thinned continental crust 30–37 km thick with the sedimentary cover up to 16 km thick. The western part of the basin was filled with sediments about 10–11 km thick and acquired the features of suboceanic crust with the Mohorovichich surface at a depth of 28–30 km with a thickness of the sedimentary cover of about 20 km.

CONFLICT OF INTEREST

The authors declare that they have no known conflicting financial interests or personal relationships that could have appeared to influence the work reported in this paper.

FUNDING

The studies were supported by the Russian Foundation of Basic Research, grant no. 20-55-56004/20.

REFERENCES

- Adamia, S.A., Chkhotia, T.G., Gavtadze, T.T., Lebanidze, Z.A., Lursmanashvili, N.D., Sadradze, N.G., Zakaria, D.P., and Zakariadze, G.S., Tectonic setting of Georgia—Eastern Black Sea: a review, in *Tectonic Evolution of the Eastern Black Sea and Caucasus*, Sosson, M., Stephenson, R.A., and Adamia, S.A., Eds., *Spec. Publ.—Geol. Soc. London*, 2017, vol. 428, pp. 11–40.
- Alavi, M., Tectonostratigraphic synthesis and structural style of the Alborz mountain system in Northern Iran, *J. Geodyn.*, 1996, vol. 21, no. 1, pp. 1–33.
- Allen, M.B., Ghassemi, M.R., Shahrabi, M., and Qorashi, M., Accommodation of late Cenozoic oblique shortening in the Alborz range, northern Iran, *J. Struct. Geol.*, 2003, vol. 25, pp. 659–672.
- Antipov, M.P., Volozh, Yu.A., Lavrushin, Yu.A., and Leonov, Yu.G., Geological events and level variations in the Caspian Sea, *Geoekologiya*, 1996, no. 3, pp. 38–50.
- Artyushkov, E.V., *Fizicheskaya tektonika* (Physical Tectonics), Moscow: Nauka, 1993 [in Russian].
- Bachmanov, D.M., Trifonov, V.G., Hessami, Kh.T., Kozhurin, A.I., Ivanova, T.P., Rogozhin, E.A., Hademi, M.C., and Jamali, F.H., Active faults in the Zagros and central Iran, *Tectonophysics*, 2004, vol. 380, pp. 221–241.
- Bank, R.A. and Neubert, E., Notes on Enidae, 7. Revision of the Enidae of Iran, with special reference to the collection of Jacques de Morgan (Gastropoda: Pulmonata), *Vita Malacologica*, 2016, vol. 14, pp. 1–84.
- Berberian, M., *Contribution on the Seismotectonics of Iran, Pt. 1*, Tehran: Geol. Surv. Iran Publ., 1976.
- Berberian, M., Qorashi, M., Jackson J.A., Priestley, K., and Wallace, T., The Rudbar-Tarom earthquake of 20 June 1990 in NW Persia: Preliminary field and seismological observation, and its tectonic significance, *Bull. Seismol. Soc. Am.*, 1992, vol. 82, no. 4, pp. 726–1755.
- Brunet, M.F., Korotaev, M.V., Ershov, A.V., and Nishin, A.M., The South Caspian Basin: a review of its evolution from subsidence modelling, *Sed. Geol.*, 2003, vol. 156, nos. 1–4, pp. 119–148.
- Danukalova, G.A., *Dvustvorchatye mollyuski i stratigrafiya akchagyla* (Bivalves and the Akchagylian stratigraphy), Moscow: Nauka, 1996 [in Russian].
- Djamour, Y., Vernant, P., Bayer, R., Nankali, H., Ritz, J.F., Hinderer, J., Hatam, Y., Luck, B., Le Moigne, N., Sedighi, M., and Khorrami, F., GPS and gravity constraints on continental deformation in the Alborz mountain range, Iran, *Geophys. J. Int.*, 2010, vol. 183, pp. 1287–1301.
- Enkin, R.J., *A Computer Program Package for Analysis and Presentation of Paleomagnetic Data*, Pacific Geosci. Centre, Geol. Surv. Canada, 1994.

- Geological Map of Iran. Sheets 2, 3. Scale 1 : 1000000*, Tehran: Nat. Iranian Oil Comp., 1977.
- Geological Map of Iran. Sheet 1. Scale 1 : 1000000*, Tehran: Nat. Iranian Oil Comp., 1978.
- Geologiya i poleznye iskopaemye Afganistana. T. 1: Geologiya (Geology and Mineral Resources of Afghanistan, Vol. 1: Geology)*, Dronov, V.I., Ed., Moscow: Недра, 1980 [in Russian].
- Ghassemi, M., Drainage evolution in response to fold growth in the hanging-wall of the Khazar fault, north-eastern Alborz, Iran, *Basin Res.*, 2005, vol. 17, pp. 425–436.
- Golubyatnikov, D.V., Oil deposits in Northern Persia, *Neft. Slants. Khoz.*, 1921, nos. 1–2, pp. 9–12.
- Guest, B., Axen, G.J., Lam, P.S., and Hassanzadeh, J., Late Cenozoic shortening in the west-central Alborz Mountains, northern Iran, by combined conjugate strike-slip and thin-skinned deformation, *Geosphere*, 2006, vol. 2, no. 1, pp. 35–52.
- Ivanova, T.P. and Trifonov, V.G., Seismotectonics and contemporary Caspian Sea level oscillations, *Geotectonics*, 2002, vol. 36, no. 2, pp. 109–123
- Jackson, J., Priestley, K., Allen, M., and Berberian, M., Active tectonics of the South Caspian Basin, *Geophys. J. Int.*, 2002, vol. 148, pp. 214–245.
- Kengerli, T.N., Aliev, F.A., Aliev, A.M., Kazimova, S.E., Safarov, R.T., and Vakhobov, U.G., Contemporary structure and active tectonics of the southern slope of Greater Caucasus within the limits of Azerbaijan (Mazymchai–Pirsaat interfluve): Pt. 1. Geological-tectonic setting, *Izv. NAN Azerbaidzhana. Ser.: Nauki Zemle*, 2018, no. 2, pp. 19–38.
- Khain, V.E., *Tektonika kontinentov i okeanov (Tectonics of Continents and Oceans)*, Moscow: Nauchn. mir, 2001 [in Russian].
- Khorrami, F., Vernant, P., Masson, F., Nilfouroushan, F., Mousavi, Z., Nankali, H., Saadat, S.A., Walpersdorf, A., Hosseini, S., Tavakoli, P., Aghamohammadi, A., and Alijanzade, M., An up-to-date crustal deformation map of Iran using integrated campaign-mode and permanent GPS velocities, *Geophys. J. Int.*, 2019, vol. 217, pp. 832–843.
- Kirschvink, J.L., The least-square line and plane and the analysis of paleomagnetic data, *Geophys. J. R. Astr. Soc.*, 1980, vol. 62, pp. 699–718.
- Knapp, C.C., Knapp, J.H., and Connor, J.A., Crustal-scale structure of the South Caspian Basin revealed by deep seismic reflection profiling, *Mar. Petrol. Geol.*, 2004, vol. 21, pp. 1073–1081.
- Knipper, A.L., Oceanic crust in the Structure of Alpine Folded Zone, in *Tr. GIN AN SSSR. Vyp. 267* (Trans. Geol. Inst. USSR Acad. Sci. Vol. 267), Moscow: Nauka, 1975 [in Russian].
- Kopp, M.L., Structures of lateral ejection in the Alpine–Himalayan collisional belt, in *Tr. GIN AN SSSR. Vyp. 506* (Trans. Geol. Inst. USSR Acad. Sci. Vol. 506), Moscow: Nauchn. Mir, 1997 [in Russian].
- Lazarev, S., Kuiper, K.F., Oms, O., Bukhsianidze, M., Vasilyan, D., Jorissen, E.L., Bouwmeester, M.J., Aghayeva, V., van Amerongen, A.J., Agusti, J., Lordkipanidze, D., and Krijgsman, W., Five-fold expansion of the Caspian Sea in the late Pliocene: New and revised magnetostratigraphic and $^{40}\text{Ar}/^{39}\text{Ar}$ age constraints on the Akchagylian Stage, *Global Planet. Change*, 2021, vol. 206, no. 103624.
- Leonov, Yu.G., Antipov, M.P., Volozh, Yu.A., Zverev, V.P., Kopp, M.L., Kostikova, I.A., and Lavrushin, Yu.A., Geological aspects of the problem of the Caspian Sea level oscillations, in *Global'nye izmeneniya prirodnoi sredy (Global Changes of the Natural Environment)*, Dobretsov, N.L., Kovalenko, V.I., Balabaev, V.T., et al., Eds., Novosibirsk: SO RAN, 1998, pp. 30–57.
- Leonov, Yu.G., Antipov, M.P., Bobylova, E.E., Volozh, Yu.A., Lavrushin, Yu.A., and Spiridonova, E.A., The 1 : 2500000 map of Quaternary (Neopleistocene) deposits of the Caspian Region with elements of paleogeography and the geological history of Quaternary sedimentary basins over the last 700 ka, in *Tr. GIN RAN. Vyp. 568* (Trans. Geol. Inst. Russ. Acad. Sci. Vol. 568), Moscow: Nauchn. Mir, 2005 [in Russian].
- Mamedov, P.Z., Contemporary structural style of the South Caspian Megabasin as a result of multistage evolution of the lithosphere in the central segment of the Alpine–Himalayan mobile belt, *Izv. NAN Azerbaidzhana. Ser.: Nauki Zemle*, 2010, no. 4, pp. 46–72.
- Moghadam, H.S. and Stern, R.J., Ophiolites of Iran: Keys to understanding the tectonic evolution of SW Asia: (I) Paleozoic ophiolites, *J. Asian Earth Sci.*, 2014, vol. 91, pp. 19–38.
- Mousavi, Z., Walpersdorf, A., Walker, R.T., Tavakoli, F., Pathier, E., Nankali, H., Nilfouroushan, F., and Djamour, Y., Global Positioning System constraints on the active tectonics of NE Iran and the South Caspian region, *Earth Planet. Sci. Lett.*, 2013, vol. 377–378, pp. 287–298.
- Nazari, H., Ritz, J.-F., and Avagyan, A., Morphotectonics and slip rate of the Khazar fault in Central Alborz (Northern Iran), *Geosciences*, 2021a, vol. 31, no. 2, pp. 101–110.
- Nazari, H., Ritz, J.-F., Burg, J.-P., Shokri, M., Haghipour, N., Mohammadi Vizheh, M., Avagyan, A., Fazeli Nashli, H., and Ensani, M., Active tectonics along the Khazar fault (Alborz, Iran), *J. Asian Earth Sci.*, 2021b, vol. 219, no. 104893, pp. 1–11.
- Patina, I.S., Leonov, Yu.G., Volozh, Yu.A., Kopp, M.L., Antipov, M.P., Trifonov, V.G., and Morozov, Yu.A., Crimea–Kopet Dagh zone of concentrated orogenic deformations as a transregional late collisional right-lateral strike-slip fault, *Geotectonics*, 2017, vol. 51, no. 4, pp. 353–365.
<https://doi.org/10.7868/S0016853X17040063>
- Popov, S.V., Golovina, L.A., and Goncharova, I.A., Miocene deposits, mollusks, and nannoplankton of the Eastern Paratethys in Northern Iran, in *Stratigraficheskie i paleogeograficheskie problemy neogena i kvartera Rossii (Stratigraphic and Paleogeographic Problems of Neogene and Quaternary of Russia)*, Moscow: GEOS, 2015, pp. 34–38.
- Popov, S.V., Golovina, L.A., Radionova, E.P., Goncharova, I.A., Filippova, N.Yu., Rostovtseva, Yu.V., and Palka, D.V., Stratotypes and reference sections of Neogene regional stages in South Russia and problems of their boundaries, in *Neogen i kvarter Rossii: stratigrafiya, sobytiya i paleogeografiya (Neogene and Quaternary of Russia: Stratigraphy, Events, and Paleogeography)*, Moscow: GEOS, 2018, pp. 47–54.
- Rashidi, A., Geometric and kinematic characteristics of the Khazar and North Alborz faults: links to the structural evolution of the North Alborz–South Caspian boundary, Northern Iran, *J. Asian Earth Sci.*, 2021, vol. 213.
<https://doi.org/10.1016/j.jseas.2021.104755>

- Rastsvetaev, L.M., Strike-slip faults and Alpine geodynamics of the Caucasus region, in *Geodinamika Kavkaza* (Geodynamics of the Caucasus), Moscow: Nauka, 1989, pp. 106–111.
- Ritz, J.F., Nazari, H., Ghassemi, A., Salamati, R., Shafei, A., Solaymani, S., and Vernant, P., Active transtention inside Central Alborz: a new insight into the Northern Iran–Southern Caspian geodynamics, *Geology*, 2006, vol. 34, no. 6, pp. 477–480.
- Saidov, M.N. and Kuchapin, A.V., *Geologicheskoe stroenie oblasti razvitiya tretichnykh otlozhenii Mazanderana (Severnyi Iran)* (Geological Structure of the Mazanderan Tertiary Deposits (Northern Iran)), Leningrad: Gostoptekhizdat, 1955 [in Russian].
- Sengör, A.M.C., The Cimmeride orogenic system and the tectonics of Eurasia, *Spec. Publ.—Geol. Soc. Am.*, 1984, vol. 195.
- Shileiko, A.A., Terrestrial Mollusks of the Suborder Pupillina of the USSR Fauna (Gastropoda, Pulmonata, Geophila), in *Fauna SSSR, Molluski, III, 3* (The Fauna of the USSR: Mollusks. Vol. III, no. 3), Leningrad: Nauka, 1984, pp. 1–399.
- Soltani, B., Beiranvand, B., Moussavi-Harami, R., Honarmand, J., and Taati, F., Facies analysis and depositional setting of the upper Pliocene Akchagyl Formation in southeastern Caspian Basin, NE Iran, *Carbonates and Evaporites*, 2020a, vol. 35, no. 8.
<https://doi.org/10.1007/s13146-019-00537-9>
- Soltani, B., Beiranvand, B., Moussavi Harami, S.R., Honarmand, J., and Taati, F., Regional factors controlling the type of Pliocene deposits in the southeastern Caspian Basin, NE Iran: Implication for tectono-stratigraphic analysis, *J. Petrol. Sci. Technol.*, 2020b, vol. 10, pp. 46–53.
<https://doi.org/10.22078/jpst.2020.4059.1648>
- Sosson, M., Rolland, Y., Mueller, C., Danelian, T., Melkonyan, R., Kekelia, S., Adamia, S., Babazadeh, V., Kangarli, T., Avagyan, A., Galoyan, G., and Mozar, J., Subductions, obduction and collision in the Lesser Caucasus (Armenia, Azerbaijan, Georgia): New insights, in *Sedimentary Basin Tectonics from the Black Sea and Caucasus to the Arabian Platform*, Sosson, M., Kaymakci, N., Stephenson, R.A., Bergerat, F., and Starostenko, V., Eds., *Spec. Publ.—Geol. Soc. London*, 2010, vol. 340, pp. 329–352.
- Stöcklin, J., Possible ancient continental margins in Iran, in *The Geology of Continental Margins*, Burk, C.A. and Drake, C.L., Eds., Berlin: Springer-Verlag, 1974, pp. 873–887.
- Svitoch, A.A., Badyukova, E.N., Sheikhi, B., and Yanina, T.A., Geological-geomorphological structure and recent history of the Iranian coast of the Caspian Sea, *Dokl. Earth Sci.*, 2013, vol. 451, no. 4, pp. 843–848.
- Svitoch, A.A., Badyukova, E.N., Yanina, T.A., and Sheikhi, B., Biostratigraphy of the Marine Holocene on the Iranian coasts of the Caspian Sea, *Quat. Int.*, 2016, vol. 409, pp. 8–15.
- Sysoev, A.V. and Schileyko, A.A., Land snails and slugs of Russia and adjacent countries, *Pensoft Ser. Faunistica*, 2009, no. 87, pp. 1–312.
- Talebian, M., Ghorashi, M., and Nazari, H., *Seismotectonic map of the Central Alborz, Scale 1 : 750000*, Geol. Surv. Iran, 2013. <http://ries.ac.ir/eqhazard/wp/Resualts.htm>
- Trifonov, V.G., Vostrikov, G.A., Lykov, V.I., Skobelev, S.F., and Orazsakhmatov, Kh., Tectonic aspects of the 1983 Kumdag earthquake, West Turkmenia, *Izv. AN SSSR. Ser. Geol.*, 1986, no. 5, pp. 3–16.
- Trifonov, V.G., Karakhanian, A.S., Berberian, M., Ivanova, T.P., Kazmin, V.G., Kopp, M.L., Kozhurin, A.I., Kuloshvili, S.I., Lukina, N.V., Mahmud, S.M., Vostrikov, G.A., Swedan, A., and Abdeen, M., Active faults of the Arabian Plate bounds in Caucasus and Middle East, *J. Earthquake Prediction Res.*, 1996, vol. 5, no. 3, pp. 363–374.
- Trifonov, V.G., Soboleva, O.V., Trifonov, R.V., and Vostrikov, G.A., *Sovremennaya geodinamika Al'piisko-Gimalaiskogo kollizionnogo poyasa* (Recent Geodynamics of the Alpine–Himalayan Collision Belt), Moscow: GEOS, 2002 [in Russian].
- Trifonov, V.G., Sokolov, S.Yu., Sokolov, S.A., and Hessami, Kh., Mesozoic–Cenozoic structure of the Black Sea–Caucasus–Caspian region and its relationships with the upper mantle structure, *Geotectonics*, 2020, vol. 54, no. 3, pp. 331–355.
<https://doi.org/10.1134/S0016852120030103>
- Ulomov, V.I., Polyakova, T.P., and Medvedeva, N.S., Seismogeodynamics of the Caspian Sea Region, *Izv., Phys. Solid Earth*, 1999, vol. 35, no. 12, pp. 1036–1042.
- Vernant, P., Nilforoushan, F., Chery, J., Bayer, R., Djamour, Y., Masson, F., Nankali, H., Ritz, J.F., Sedighi, M., and Tavakoli, F., Deciphering oblique shortening of central Alborz in Iran using geodetic data, *Earth Planet. Sci. Lett.*, 2004, vol. 223, pp. 177–185.
- Vlaminck, S., Kehl, M., Lauer, T., Shahriari, A., Sharifi, J., Eckmeier, E., Lehndorff, E., Khormali, F., and Frechen, M., Loess-soil sequence at Toshan (Northern Iran): Insights into late Pleistocene climate change, *Quat. Int.*, 2016, vol. 399, pp. 122–135.
- Wang, X., Wei, H., Taheri, M., Khormali, F., Danukalova, G., and Chen, F., Early Pleistocene climate in western arid central Asia inferred from loess-palaeosol sequences, *Sci. Rep.*, 2016, vol. 6, no. 20560.
- Zanchi, A., Berra, F., Mattei, M., Ghassemi, M., and Sabouri, J., Inversion tectonics in central Alborz, Iran, *J. Structural Geol.*, 2006, vol. 28, pp. 2023–2037.